Matter-wave solitons in heteronuclear atomic Bose-Einstein condensates with synchronously controllable interactions and potentials

Cai-Ying Ding,[1] Xiao-Fei Zhang,[2] Dun Zhao,[1,3] Hong-Gang Luo,[1,4,*] and W. M. Liu[2]

[1]*Center for Interdisciplinary Studies & Key Laboratory for Magnetism and Magnetic Materials of the MoE, Lanzhou University, Lanzhou 730000, China*

[2]*Beijing National Laboratory for Condensed Matter Physics, Institute of Physics, CAS, Beijing 100190, China*

[3]*School of Mathematics and Statistics, Lanzhou University, Lanzhou 730000, China*

[4]*Beijing Computational Science Research Center, Beijing 100084, China*

(Received 20 August 2011; published 28 November 2011)

We investigate exact matter-wave soliton pairs of two-component heteronuclear atomic Bose-Einstein condensates with tunable interactions and harmonic potentials by using a combination of the homogeneous balance principle and the F-expansion technique. Our results show that exact matter-wave soliton pairs are asymmetric where their existence requires some restrictive conditions corresponding to experimentally controllable interactions and harmonic potential parameters. In contrast to homonuclear systems, the potentials for two components in heteronuclear systems are different, which is due to the mass of two components being unequal. Considering two explicit situations of the interaction parameters, we further explore the collision dynamics of the soliton pairs with opposite velocities by synchronously controlling the interaction and potential parameters. The collision dynamics occur during and after the simultaneous evaporative cooling of two condensates. The results show that collisions are elastic and that the solitons after the collision can keep their identities. In addition, we find that the amplitudes of the soliton pairs periodically grow with time during the cooling process and, for the same initial conditions, the collision time of the soliton pair without gain is delayed compared with that with gain. We also discuss how to observe these new phenomena in future experiments.

DOI: 10.1103/PhysRevA.84.053631 PACS number(s): 03.75.Mn, 03.75.Lm, 05.45.Yv

I. INTRODUCTION

Since the experimental realizations of Bose-Einstein condensates (BECs) for rubidium and sodium in 1995 [1], the study of the properties of these systems has attracted a great deal of attention. In recent years, more interest has been focused on the dynamics of the multiple-component mixtures. Different from the single-component BECs, the mixtures of two species exhibit many remarkable phenomena such as phase separation [2–5] and different combinations of the various soliton pairs [6–11], which are unavailable in the single-component BECs. With the development of technology, the dynamics of the BECs can be controlled by adjusting the harmonic traps confining the BECs and/or by tuning the nonlinear interactions via the Feshbach resonance technique [12–16]. In the case of two-component BECs, the interactions include intra- and interspecies interactions and they can been tuned independently in experiments [17].

According to the type of atoms making up the BECs, two-component BECs can be divided into two categories: one is a homonuclear mixture such as that of two hyperfine states of ^{87}Rb [18], and the other is a heteronuclear mixture where the different atomic species [16,19–23], or different isotopes of the same atomic species [15] are populated. In some recent works the dynamics of two-component systems has been investigated by considering time- and/or space-dependent interactions and a time-dependent harmonic external potential [24–27]. In addition, two matter-wave bright soliton solutions of the coupled nonlinear Schrödinger (NLS) equations with a spatial-modulating nonlinearity are also given and their dynamical behavior has been explored [28] using a variational approach. All these works were limited to homonuclear atomic systems. For the heteronuclear case, the two components of the BECs are asymmetric. In this situation, the soliton dynamics of the BECs with time-dependent coefficients has not been reported in the literature.

The aim of this paper is to study exact soliton pairs and the collision dynamics of two-component heteronuclear atomic BECs. The exact soliton can be obtained by a combination of the homogeneous balance principle and the F-expansive technique [29–32]. The result shows that these soliton pairs are asymmetric and that they exist only under a set of restrictive conditions in which the interaction, harmonic potential, and gain (or loss) [33] parameters are dependent on each other; and the first two types of parameters are synchronously controllable in experiments. In addition, the harmonic potentials for different components are also different. We consider two explicit time-dependent-interaction cases: one is where all interactions vary homogeneously and the other is when the "intra" interactions are fixed and "inter" interactions are time-dependent. In these cases, we explore the soliton collision dynamics with or without gain by synchronous control over the interactions and the harmonic potentials. The results show that the condensates grow periodically with modulations of two types of parameters during the simultaneous evaporative cooling, and the collision time of two solitons is delayed without cooling when compared with that during cooling for the same initial conditions. Moreover, collisions between solitons are basically elastic. These phenomena are expected to be observed in future experiments.

*luohg@lzu.edu.cn

II. HETERONUCLEAR TWO-COMPONENT SYSTEM AND ITS EXACT SOLITON-PAIR SOLUTIONS

We consider a two-species interacting atomic BEC trapped in external potentials during the simultaneous evaporative cooling process. In the zero-temperature approximation, the systems can be well described by the following coupled NLS equations:

$$\begin{aligned} i\hbar\frac{\partial\Psi_1}{\partial t} &= \left(-\frac{\hbar^2\nabla^2}{2m_1}+U_{11}|\Psi_1|^2+U_{12}|\Psi_2|^2\right)\Psi_1 \\ &\quad +\left(V_{\rm ext}^{(1)}+i\hbar\Gamma_1\right)\Psi_1, \\ i\hbar\frac{\partial\Psi_2}{\partial t} &= \left(-\frac{\hbar^2\nabla^2}{2m_2}+U_{21}|\Psi_1|^2+U_{22}|\Psi_2|^2\right)\Psi_2 \\ &\quad +\left(V_{\rm ext}^{(2)}+i\hbar\Gamma_2\right)\Psi_2, \end{aligned}$$

where the condensate wave functions are normalized by the particle numbers $N_i=\int d^3\mathbf{r}|\Psi_i|$ $(i=1,2)$, and $U_{ii}=4\pi\hbar^2a_{ii}/m_i$ and $U_{12}=U_{21}=2\pi\hbar^2a_{12}/m_R$ represent intraspecies and interspecies interactions strengths, respectively, with $a_{ij}(j=1,2)$ being the corresponding scattering lengths and $m_R=m_1m_2/(m_1+m_2)$. The external trapped potentials are assumed to be $V_{\rm ext}^{(i)}=m_i[\omega_{ix}^2x^2+\omega_{i\perp}^2(y^2+z^2)]/2$. Here we assume that the condensates are trapped in elongated and regulatable harmonic oscillating external potentials; namely, $\omega_{i,\perp}\gg\omega_{i,x}$, which means that their transverse motion is frozen to the ground state of the transverse harmonic trapping potentials. Γ_i are gain (or loss) terms which give rise to the growth of the two condensates and which can be used to describe the evaporative cooling process.

Hence the system is quasi-one-dimensional. Integrating out the transverse coordinates, the resulting equations for the axial wave functions $\psi_i(x,t)$ in dimensionless form can be written as

$$\begin{aligned} i\frac{\partial\psi_1}{\partial t} &= -\frac{1}{2}\frac{\partial^2\psi_1}{\partial x^2}+(g_{11}|\psi_1|^2+g_{12}|\psi_2|^2)\psi_1 \\ &\quad +\frac{\lambda_1^2}{2}x^2\psi_1+i\gamma_1\psi_1, \qquad (1) \\ i\frac{\partial\psi_2}{\partial t} &= -\frac{\kappa}{2}\frac{\partial^2\psi_2}{\partial x^2}+(g_{21}|\psi_1|^2+g_{22}|\psi_2|^2)\psi_2 \\ &\quad +\frac{\lambda_2^2}{2}x^2\psi_2+i\gamma_2\psi_2, \qquad (2) \end{aligned}$$

where x and t are the spatial and temporal coordinates measured in units $a_0=\sqrt{\hbar/(m_1\omega_{1\perp})}$ and $\omega_{1\perp}^{-1}$, respectively. The other parameters in Eqs. (1) and (2) are defined as $g_{11}=2a_{11}$, $g_{22}=2a_{22}m_1\eta/m_2$, $g_{12}=g_{21}=2m_1a_{12}/[(1+\eta)m]$, $\eta=\omega_{2\perp}/\omega_{1\perp}$, $\lambda_i=\omega_{ix}/\omega_{1\perp}$, $\gamma_i=\Gamma_i/\omega_{1\perp}$, and $\kappa=m_1/m_2$. In addition, a_{11}, a_{22}, a_{12}, λ_i, and γ_i are controllable time-dependent parameters in experiments.

In previous works, for the interaction parameters the symmetric cases including $g_{11}(t)=g_{22}(t)=g_{12}(t)$ and $g_{11}(t)=g_{22}(t)\neq g_{12}(t)$ and the asymmetric case $g_{11}(t)\neq g_{22}(t)\neq g_{12}(t)$ have been studied extensively in homonuclear systems such as two hyperfine spin states of ^{87}Rb in Ref. [24,26], where all interactions are thought to be equal due to the small differences between them. In Ref. [24], the interaction between solitons was realized by modulating the atomic interactions via the Feshbach resonance technique and with a fixed external potential, while in Ref. [26] the dynamics of solitons evolves by synchronous modulation of the interaction and external potential. For the heteronuclear systems and considering only time-independent interactions, various soliton-pair solutions with unchanged amplitudes and speeds have been obtained. When these soliton pairs are taken as the initial profiles of the matter waves, their evolution has also been studied numerically by Feshbach resonance management [10]. Here we consider the same heteronuclear systems but with time-dependent interactions and external potentials. In the following we directly solve the most general coupled NLS equations with distributed coefficients used to describe the systems and obtain exact soliton-pair solutions. As a starting point, we take the following ansatz as the most general solution of the NLS equations (1) and (2):

$$\begin{aligned} \psi_1(x,t) &= A_1(x,t)e^{iB_1(x,t)}, \\ \psi_2(x,t) &= A_2(x,t)e^{iB_2(x,t)}, \end{aligned} \qquad (3)$$

where $A_i(x,t)$ and $B_i(x,t)$ $(i=1,2)$ are real functions of x and t. Substituting Eq. (3) into Eqs. (1) and (2), one can obtain the following equations for A_i and B_i:

$$0=\frac{\partial A_1}{\partial t}+\frac{\partial A_1}{\partial x}\frac{\partial B_1}{\partial x}+\frac{1}{2}A_1\frac{\partial^2B_1}{\partial x^2}-\gamma_1(t)A_1, \qquad (4)$$

$$\begin{aligned} 0 &= -A_1\frac{\partial B_1}{\partial t}+\frac{1}{2}\frac{\partial^2A_1}{\partial x^2}-\frac{1}{2}A_1\left(\frac{\partial B_1}{\partial x}\right)^2-g_{11}(t)A_1^3 \\ &\quad -g_{12}A_2^2A_1-\frac{1}{2}\lambda_1^2(t)x^2A_1, \qquad (5) \end{aligned}$$

$$0=\frac{\partial A_2}{\partial t}+\kappa\frac{\partial A_2}{\partial x}\frac{\partial B_2}{\partial x}+\frac{\kappa}{2}A_2\frac{\partial^2B_2}{\partial x^2}-\gamma_2(t)A_2, \qquad (6)$$

$$\begin{aligned} 0 &= -A_2\frac{\partial B_2}{\partial t}+\frac{\kappa}{2}\frac{\partial^2A_2}{\partial x^2}-\frac{\kappa}{2}A_2\left(\frac{\partial B_2}{\partial x}\right)^2-g_{22}(t)A_2^3 \\ &\quad -g_{12}A_1^2A_2-\frac{1}{2}\lambda_2^2(t)x^2A_2. \qquad (7) \end{aligned}$$

Based on the homogeneous balance principle [29] and the F-expansion technique [30], we set $A_i(x,t)=f_i(t)F(\theta)+g_i(t)/F(\theta)$ with $\theta=k(t)x+\omega(t)$. Here $k(t)$ and $\omega(t)$ are the inverse spatial width and velocity of the wave, respectively. The functions $f_i(t)$ and $g_i(t)$ are parameters to be determined below. In the expressions for A_i, $F(\theta)$ denotes a Jacobi elliptic function, which satisfies the following first-order nonlinear ordinary differential equation:

$$\left(\frac{dF(\theta)}{d\theta}\right)^2=c_0+c_2F(\theta)^2+c_4F(\theta)^4, \qquad (8)$$

where c_0, c_2, and c_4 are real constants related to the elliptic modulus m of the Jacobi elliptic functions (JEFs; see Table I). In addition, it is assumed that $B_i(x,t)=a_i(t)x^2+b_i(t)x+e_i(t)$, where a_i, b_i, and e_i are time-dependent chirp functions, wave numbers, and phase shifts, respectively, which will be determined self-consistently. Then we substitute the expressions of A_i and B_i into Eqs. (4)–(7) and collect the coefficients of the polynomial $x^pF(\theta)^q$, where p and q are nonnegative integers. One can determine those parameters included in the

TABLE I. All possible Jacobi elliptic functions (JEFs, fifth column) satisfy Eq. (8), in which the values of c_0, c_2 and c_4 are determined uniquely for a given JEF form. Here m denotes the elliptic modulus of the JEFs. The last two columns represent the limiting cases of the JEFs. When $m \to 0$, the JEFs reduce to the trigonometric functions and when $m \to 1$, the JEFs become hyperbolic functional forms or unity (the last two cases).

	c_0	c_2	c_4	$F(\theta)$	$m=0$	$m=1$
1	1	$-(1+m)$	m	sn	sin	tanh
2	$1-m$	$2m-1$	$-m$	cn	cos	sech
3	$m-1$	$2-m$	-1	dn	1	sech
4	m	$-(1+m)$	1	ns	cosec	coth
5	$-m$	$2m-1$	$1-m$	nc	sec	cosh
6	-1	$2-m$	$m-1$	nd	1	cosh
7	1	$2-m$	$1-m$	sc	tan	sinh
8	$1-m$	$2-m$	1	cs	cot	csch
9	1	$-(1+m)$	m	cd	cos	1
10	m	$-(1+m)$	1	dc	sec	1

expressions of $A_i(x,t)$ and $B_i(x,t)$ by taking the coefficients of $F(\theta)$ as zero:

$$\begin{aligned} k(t) &= D_1 e^{-2\int a(t)dt}, \\ \omega(t) &= -D_2 D_1 \int e^{-4\int a(t)dt} dt + D_4, \\ b_1(t) &= D_2 e^{-2\int a(t)dt}, \quad b_2(t) = \frac{b_1(t)}{\kappa}, \\ f_i(t) &= D_{3i} e^{\int [\gamma_i(t) - a(t)]dt}, \\ g_i(t) &= D_{5i} e^{\int [\gamma_i(t) - a(t)]dt}, \\ e_i(t) &= \int h_i(t) e^{-2\int a(t)dt} dt, \end{aligned} \tag{9}$$

where $a(t) = a_1(t) = \kappa a_2(t)$ are the chirp functions. D_1 and D_{3i} $(i = 1,2)$ are real constants and represent the initial inverse spatial width and the initial amplitudes of the waves, respectively. D_2 and D_4 are arbitrary real constants. The value of D_{5i} will be discussed for the case of soliton solutions (see below). In addition, the expressions of $h_i(t)$ in the phase shifts are given by

$$\begin{aligned} h_1(t) &= D_{11} g_{12}(t) e^{2\int \gamma_2(t)dt} - 3 D_{51} D_{31} g_{11}(t) e^{2\int \gamma_1(t)dt} \\ &\quad + \frac{1}{2}\left(c_2 D_1^2 - D_2^2\right) e^{-2\int a(t)dt}, \\ h_2(t) &= D_{22} g_{12}(t) e^{2\int \gamma_1(t)dt} - 3 D_{32} D_{52} g_{22}(t) e^{2\int \gamma_2(t)dt} \\ &\quad + \frac{\kappa}{2}\left(c_2 D_1^2 - \frac{D_2^2}{\kappa^2}\right) e^{-2\int a(t)dt}. \end{aligned} \tag{10}$$

Here one defines $D_{11} = -D_{32}(2D_{52}D_{31} + D_{32}D_{51})/D_{31}$ and $D_{22} = -D_{31}(2D_{32}D_{51} + D_{52}D_{31})/D_{32}$.

Furthermore, it is worth noting that the chirp function satisfies the following standard Ricatti-type equation:

$$\frac{da(t)}{dt} + 2a^2(t) + \frac{\lambda^2(t)}{2} = 0, \tag{11}$$

with $\lambda(t) = \lambda_1(t) = \kappa\lambda_2(t)$. It can thus be seen that the external potentials for the two components are significantly different in heteronuclear systems, which is caused by the mass of two components being different. In homonuclear systems, due to the mass ratio of the two components being unity (i.e., $\kappa = 1$), then the potentials for the two components are identical.

At the same time, the existence of exact solutions requires a set of constraint conditions:

$$D_{3i}^2 e^{2\int [\gamma_i(t) - a(t)]dt} = c_4 \Delta_i k(t)^2, \tag{12}$$

$$D_{5i}^2 e^{2\int [\gamma_i(t) - a(t)]dt} = \epsilon^2 c_0 \Delta_i k(t)^2, \tag{13}$$

where $\epsilon = 0, \pm 1$ and

$$\Delta_1 = \frac{g_{22}(t) - \kappa g_{12}(t)}{g_{22}(t)g_{11}(t) - g_{12}(t)g_{21}(t)}, \tag{14}$$

$$\Delta_2 = \frac{\kappa g_{11}(t) - g_{12}(t)}{g_{22}(t)g_{11}(t) - g_{12}(t)g_{21}(t)}. \tag{15}$$

The similar conditions are usually called integrable conditions [31], which are quite complicated in the general case. From Table I, Eqs. (1) and (2) have various solutions. When $0 < m < 1$, the JEFs are periodic traveling wave solutions. When $m \to 0$, the periodic traveling wave solutions evolve into the periodic trigonometric functions. When $m \to 1$, the periodic traveling wave solutions become the time-dependent soliton solutions of the coupled NLS equations.

In the following, we mainly focus on the soliton solutions by taking the elliptic modulus m as 1. According to the conditions of Eqs. (12) and (13), c_0, c_4, and Δ_i take the same sign. After some careful analysis, we find that only the first three lines in Table I are able to give out soliton-pair solutions. In the first line of Table I, because $c_0 \neq 0$ and $F(\theta)$ has the tanh form, one takes $\epsilon = 0$ to avoid a possible divergence caused by $1/F(\theta)$ in the second term of $A_i(x,t)$. As a consequence, D_{5i} are zero, thus g_i are zero, and a dark-dark soliton-pair solution can be obtained. In the second and third lines, because c_0 is zero, the values of D_{5i} are bound to zero according to the condition of Eq. (13) and a bright-bright soliton-pair solution is obtained. Thus, for these two classes of soliton-pair solutions, only Eq. (12) survives, which is the so-called integrable condition in the present paper. Finally, two types of soliton-pair solutions can be written as

$$\begin{aligned} \psi_1(x,t) &= f_1(t) F(\theta) e^{i[a(t)x^2 + b_1(t)x + e_1(t)]}, \\ \psi_2(x,t) &= f_2(t) F(\theta) e^{i[a(t)x^2 + b_2(t)x + e_2(t)]}. \end{aligned} \tag{16}$$

For these two types of soliton-pair solutions, Eq. (12) proposes explicit constraint conditions on the interaction parameters g_{ij} and κ, as shown in Table II. Note that, for the heteronuclear system, the phase shifts for the two components are different, which is in contrast to the case of homonuclear systems. We thus obtain the symbiotic solitons in heteronuclear two-component systems with the time-dependent interactions and external potentials. Considering the possible preparation in experiments, we can first load the two condensates into the harmonic cigar trap (during the simultaneous evaporative cooling of a mixture of two gases, with this case corresponding to $\gamma \neq 0$). Then we use techniques like phase imprinting to prepare the initial soliton pair and change the trap frequencies, together with the scattering lengths changed by the Feshbach resonance, according to Eq. (11) and the integrable conditions of Eq. (12). The bright-bright or dark-dark soliton with time-varying amplitudes and speeds may appear in the systems.

TABLE II. Explicit constraint conditions on the "intra" and "inter" interactions and the parameter κ for the bright-bright and dark-dark soliton-pair solutions and their phase shifts.

Soliton pairs	Existence	Phase shifts
Bright-bright	$g_{22} < \kappa g_{12}, \kappa g_{11} < g_{12}, g_{22}g_{11} > g_{12}^2$ or $g_{22} > \kappa g_{12}, \kappa g_{11} > g_{12}, g_{22}g_{11} < g_{12}^2$	$e_1(t) = \frac{1}{2}\left(D_1^2 - D_2^2\right)\int e^{\int -4a(t)dt}dt$ $e_2(t) = (\kappa/2)\left(D_1^2 - D_2^2/\kappa^2\right)\int e^{\int -4a(t)dt}dt$
Dark-dark	$g_{22} < \kappa g_{12}, \kappa g_{11} < g_{12}, g_{22}g_{11} < g_{12}^2$ or $g_{22} > \kappa g_{12}, \kappa g_{11} > g_{12}, g_{22}g_{11} > g_{12}^2$	$e_1(t) = -\left(D_1^2 + D_2^2/2\right)\int e^{\int -4a(t)dt}dt$ $e_2(t) = -\kappa\left(D_1^2 + D_2^2/2\kappa^2\right)\int e^{\int -4a(t)dt}dt$

Hence their dynamical behavior can be controlled by tuning experimentally the interaction and harmonic external potential parameters under the constraint conditions, which is explicitly discussed later.

III. DISCUSSION OF INTEGRABLE CONDITION

The integrable condition Eq. (12) provides many possibilities to tune the interaction and external potential parameters. According to the condition, a relationship between two components can be written as

$$\frac{\Delta_1}{\Delta_2} = \frac{D_{31}^2}{D_{32}^2} e^{2\int[\gamma_1(t)-\gamma_2(t)]dt}, \tag{17}$$

from which one can conclude that Δ_1 and Δ_2 have the same sign. In the following we explicitly discuss two classes of interaction parameter cases.

First, we consider that all interaction parameters are tuned homogeneously; namely, $g_{11}(t) = \delta_{11}g_0(t)$, $g_{22}(t) = \delta_{22}g_0(t)$, and $g_{12}(t) = \delta_{12}g_0(t)$, where δ_{11}, δ_{22}, and δ_{12} are time-independent interaction parameters dependent on the explicit systems and $g_0(t)$ is a modulated interaction parameter. In this case, Eqs. (14) and (15) can be simplified to

$$\begin{aligned} \Delta_1 &= \frac{1}{g_0(t)}\frac{\delta_{22} - \kappa\delta_{12}}{\delta_{22}\delta_{11} - \delta_{12}^2}, \\ \Delta_2 &= \frac{1}{g_0(t)}\frac{\kappa\delta_{11} - \delta_{12}}{\delta_{22}\delta_{11} - \delta_{12}^2}. \end{aligned} \tag{18}$$

In addition, the initial amplitudes of soliton pairs can be identified as $D_{31}^2 = c_4\Delta_1 g_0(t)D_1^2$ and $D_{32}^2 = c_4\Delta_2 g_0(t)D_1^2$. After these parameters are given, Eqs. (11) and (12) can be recombined into

$$-\frac{g_{0,tt}}{g_0} + 2\frac{g_{0,t}}{g_0} - 2\gamma_t + 4\gamma^2 g_0^2 + 4\frac{\gamma g_{0,t}}{g_0} + \lambda^2 = 0. \tag{19}$$

The subscript "t" denotes differentiation with respect to time. This is a condition under which the soliton-pair solutions can exist when the interaction and external potential parameters are time dependent.

As the second case, we let $g_{11}(t) = \delta_{11}$ and $g_{22}(t) = \delta_{22}$ be real constants and $g_{12}(t) = g_{21}(t) = g(t)$ are time-dependent. These correspond to the inhomogeneous case. Then one has

$$\begin{aligned} \Delta_1 &= \frac{\kappa}{\kappa\delta_{11} + g(t)}, \\ \Delta_2 &= \frac{1}{\kappa\delta_{11} + g(t)}, \end{aligned} \tag{20}$$

and $\delta_{22} = \kappa^2\delta_{11}$. Moreover, we take the constant amplitudes of soliton pairs $D_{31}^2 = c_4\kappa D_1^2$ and $D_{32}^2 = c_4 D_1^2$. As a result, Eqs. (11) and (12) can be merged into

$$\begin{aligned} \lambda^2(t) = 2\gamma_t - \frac{g_t^2}{[\kappa\delta_{11} + g(t)]^2} + \frac{g_{tt}}{\kappa\delta_{11} + g(t)} \\ - \left[2\gamma + \frac{g_t}{\kappa\delta_{11} + g(t)}\right]^2. \end{aligned} \tag{21}$$

Likewise, this is a condition under which the soliton-pair solutions exist. In the above cases, $\gamma_1 = \gamma_2 = \gamma$ can be obtained from Eq. (17). In the following section we discuss explicit collision dynamics of the soliton pairs under these conditions.

IV. COLLISION DYNAMICS OF SOLITON PAIRS

Interactions between two solitons can exhibit a very intriguing collision dynamics behavior, like particles which preserve their identify after passing through each other. For same-atom systems the collision is, in essence, partially coherent due to a direct overlapping of the atoms but, for different atoms, due to the incoherent nature, the collision is incoherent, which is the case we study here. In this situation, the total intensity of two solitons is $I = |\psi_1|^2 + |\psi_2|^2$. Explicitly, we investigate the elastic collisions of soliton pairs with opposite velocities by synchronizing control over the interactions and external potentials mentioned above. For comparison, we consider two experimentally accessible systems to study the influence on the soliton-pair collision dynamics of related parameters that are tuned experimentally.

A. Case of homogeneously tuned interactions

As the first case, we consider that all interaction parameters are modulated periodically by the Feshbach resonance technique according to

$$g_0(t) = 1 + A\sin(\Omega t), \tag{22}$$

where A and Ω are the amplitude and frequency of the modulation and here we take $A = 0.7$ and $\Omega = 0.25$. Using this modulation we investigate the collision dynamics of two types of soliton pairs for the special system of an ^{87}Rb-^{41}K mixture with the dimensionless parameters $\delta_{11} = 69$ and $\delta_{22} = 99$ during simultaneous evaporative cooling. Here and hereafter, all parameters are dimensionless. According to Table I and the definition of the initial amplitudes, the

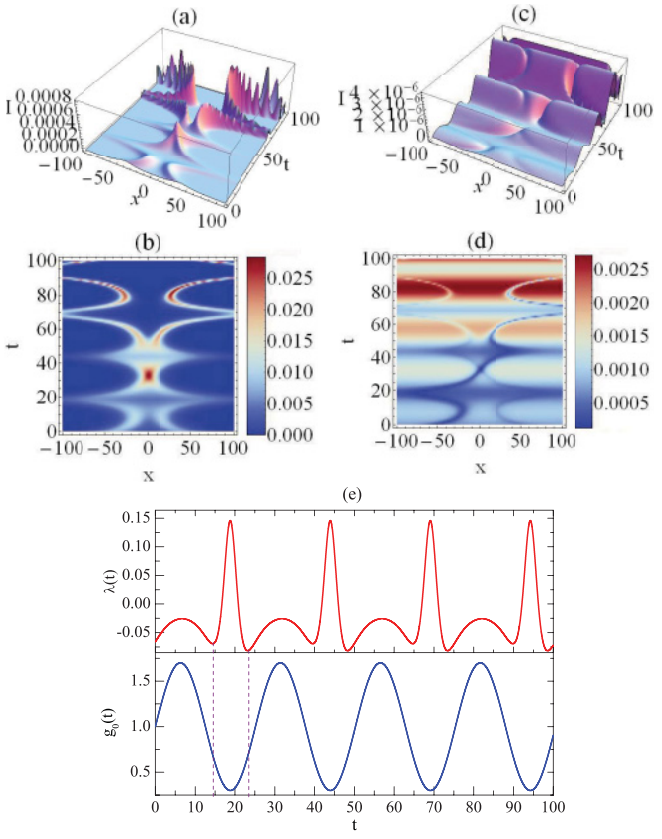

FIG. 1. (Color online) Elastic collision dynamics of bright-bright and dark-dark soliton pairs with opposite velocities, and synchronous evolution of external potential with modulation of homogeneous interaction via Feshbach resonance in ^{87}Rb-^{41}K mixture with growth of condensates. The parameters used are given by $A = 0.7, \Omega = 1/4$, $\gamma = 1/150$, and $D_4 = 4$. (a) Collision dynamics of bright-bright soliton pair with $D_1 = 1/150$, $D_2 = 1/20$, $c_2 = 1$, and $c_4 = -1$. (b) Corresponding density plot for Fig. 1(a). (c) Collision dynamics of dark-dark soliton pair with $D_1 = 1/200$, $D_2 = 1/15$, $c_2 = -2$, and $c_4 = 1$. (d) Corresponding density plot of Fig. 1(c). (e) Synchronous controls of the external harmonic potential (upper panel) with the homogenous interaction (lower panel).

existence of a bright-bright soliton pair requires $\Delta_1 < 0$ and $\Delta_2 < 0$. Hence we take $\delta_{12} = -84$. The chosen parameters are related to those used in previous work [8], where $g_0(t) = 1$ was assumed and the bright-bright soliton pair with constant velocities, amplitudes, and widths formed as a consequence of modulation instability (MI). In our work, the collision dynamics of the bright-bright soliton pair is shown in Fig. 1(a). It is found that the solitons pass through each other after merging at about $t = 30$, as also shown in Fig. 1(b) for a corresponding density plot. In this process, the solitons oscillate and deform due to the synchronous modulation of the homogeneous interaction parameters and the external potentials, which are shown in Fig. 1(e).

Next we study the dark-dark soliton and consider the same physical system and parameters δ_{11}, δ_{22} as for the bright-bright-soliton pair. In this situation, $\Delta_1 > 0$ and $\Delta_2 > 0$ are necessary for the existence of the dark-dark soliton pair. So we set $\delta_{12} = 200$ to meet the requirements. Shown in Figs. 1(c) and 1(d) is the collision scene between the dark-dark soliton pair, which is obviously elastic.

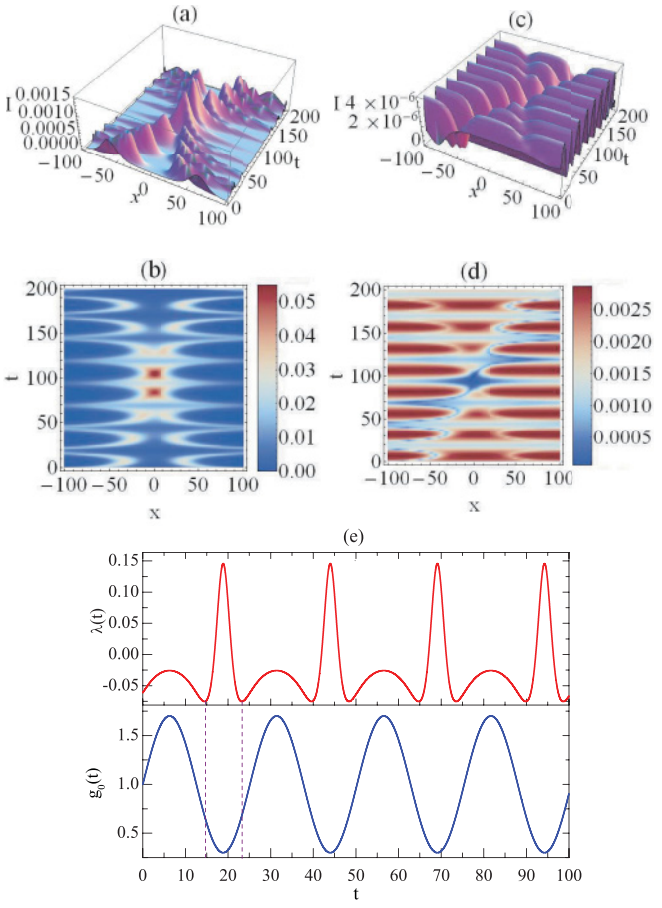

FIG. 2. (Color online) Collision dynamics between soliton pairs and evolution of external potential after evaporative cooling. The parameters used are $D_4 = 4$, and $\gamma = 0$ for the collision dynamics of the bright-bright soliton pair [(a) and (b)] and the dark-dark soliton pair [(c) and (d)]. (e) Synchronous control of the external potential (upper panel) with homogenous interaction (lower panel). The other parameters used are the same as for Fig. 1.

In the above case, the MI also occurs for the existence of the two types of solitons. From Fig. 1, it is easy to see that each soliton pair is sharply asymmetric due to the mass ratio of two components and because $\delta_{11} \neq \delta_{22} \neq \delta_{12}$, and their amplitudes grow periodically with time along their propagation directions. In addition, the growth of the two condensates in each period makes the depth of the potential well shallow in order to keep the basic excitation of the two condensates unchanged, which leads to two asymmetric dips of the strength of the external potential around $t = 15$ and $t = 25$. From the upper panel of Fig. 1(e), the potential well [$\lambda(t) > 0$] and barrier [$\lambda(t) < 0$] alternate with the periodic modulation of the homogeneous interaction parameter. Furthermore, Eq. (19) shows that the strength only depends on the time-dependent interaction and the gain term, but has nothing to do with the constant interaction parameters in the two-component BECs and their mass ratio. Thus the evolution behavior of the strengths for different soliton pairs is identical under the modulation of the same homogeneous interaction and gain term.

Finally, we study the collision dynamics of such soliton pairs without evaporative cooling (in this case, $\gamma = 0$) by controlling the homogeneous interaction parameter as

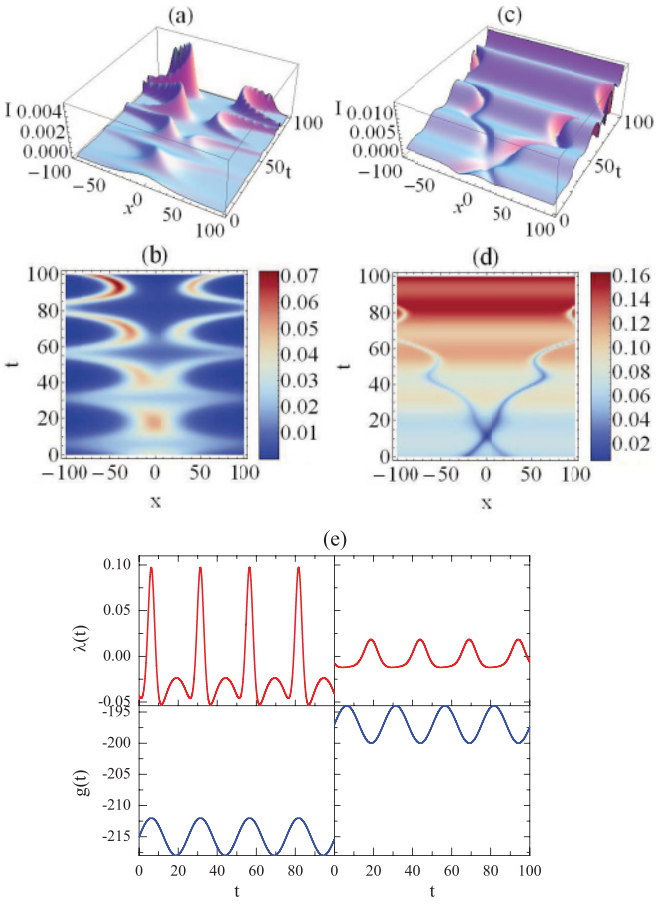

FIG. 3. (Color online) Collision dynamics between soliton pairs under interspecies interactions via Feshbach resonance management and synchronous evolution of time-dependent external potentials in ^{87}Rb-^{41}K mixture with growth of condensates. The parameters used are $\gamma = 1/200$, $\Omega = 1/4$, $A = 3$, $D_1 = 1/6000$, and $D_2 = 1/400$. (a) Collision dynamics of bright-bright soliton pair with $D_4 = 1$ and $\xi = -215$. (b) Corresponding density plot for Fig. 3(a). (c) Collision dynamics of dark-dark soliton pair with $D_4 = 8$ and $\xi = -197$. (d) Corresponding density plot for Fig. 3(c). (e) Synchronous controls of external harmonic potential and interaction for bright-bright soliton (left panel) and dark-dark soliton pairs (right panel).

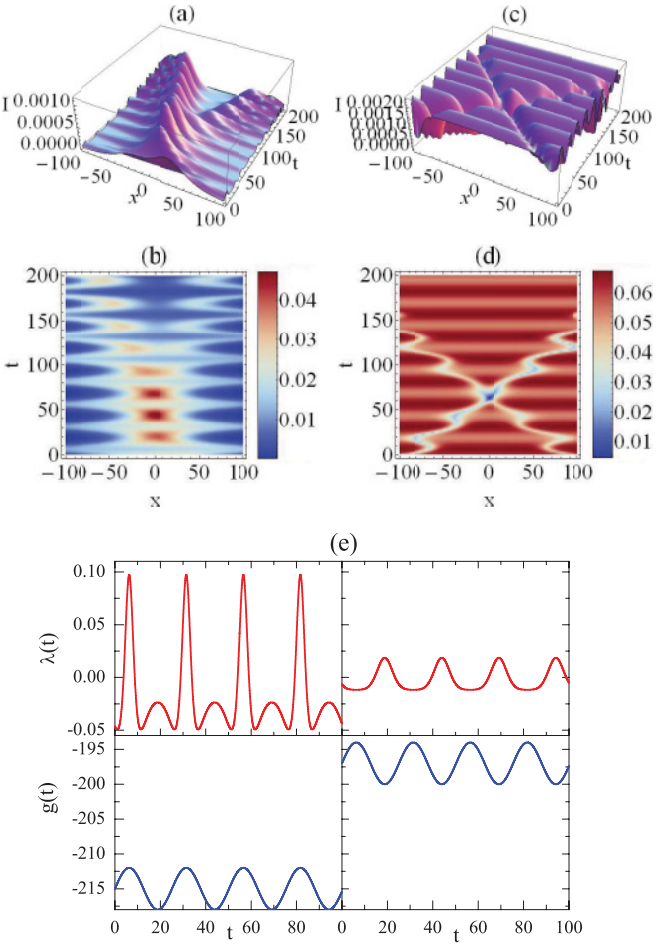

FIG. 4. (Color online) Collision dynamics between soliton pairs and synchronous change with time of external potentials in absence of gain term. The parameters are as follows: Panels (a) and (b) show the collision dynamics of the bright-bright pair with $D_4 = 1$ and $\xi = -215$. Panels (c) and (d) show the collision dynamics of the dark-dark pair with $D_4 = 8$ and $\xi = -197$. (e) Synchronous controls of the external harmonic potential and the interaction for the bright-bright soliton (left panel) and the dark-dark soliton pairs (right panel). The other parameters used are the same as for Fig. 3.

mentioned above and as shown in Fig. 2. Comparison of the condensates during the simultaneous evaporation shows that the peak density of each soliton in adjacent periods is the same in the absence of condensate growth, and the strength of the harmonic external potential is perfectly symmetric at each period, as shown at the top of Fig. 2(e). Moreover, it is found that the collision times of soliton pairs without a gain term are delayed in the same initial conditions.

B. Inhomogeneous case

Next we consider the case with fixed intraspecies interactions, but with a time-dependent interspecies interaction modulated as

$$g(t) = \xi + A\sin(\Omega t). \tag{23}$$

Here we take the modulation amplitude $A = 3$ and Ω to be the same as above. According to these values and the existence conditions [i.e., $\kappa\delta_{11} < -g(t)$ for the bright-bright solitons pair and $\kappa\delta_{11} > -g(t)$ for dark-dark soliton pair], ξ is different for the former and for the latter in explicit systems. The modulation type is easy to realize under the present experimental condition for the heteronuclear system of an ^{87}Rb-^{41}K mixture [16].

In this system, when $\delta_{11} = 99$ for a ^{87}Rb atom, it requires $\delta_{22} = \kappa^2\delta_{11} \sim 446$ for ^{41}K. ξ is taken to be -215 for the bright-bright soliton pair and -197 for the dark-dark soliton pair. Under synchronous modulation of the interspecies interactions and external potentials, the collision dynamics of the bright-bright and dark-dark soliton pairs are shown in Figs. 3(a)–3(d) with the gain terms and in Figs. 4(a)–4(d) with no gain terms. Figures 3(e) and 4(e) show the synchronous behavior of the time-dependent external potentials for the bright-bright soliton-pair dynamics (left) and the dark-dark soliton-pair dynamics (right). With the same initial conditions, the collision times are also delayed in Figs. 4(a)–4(d) compared

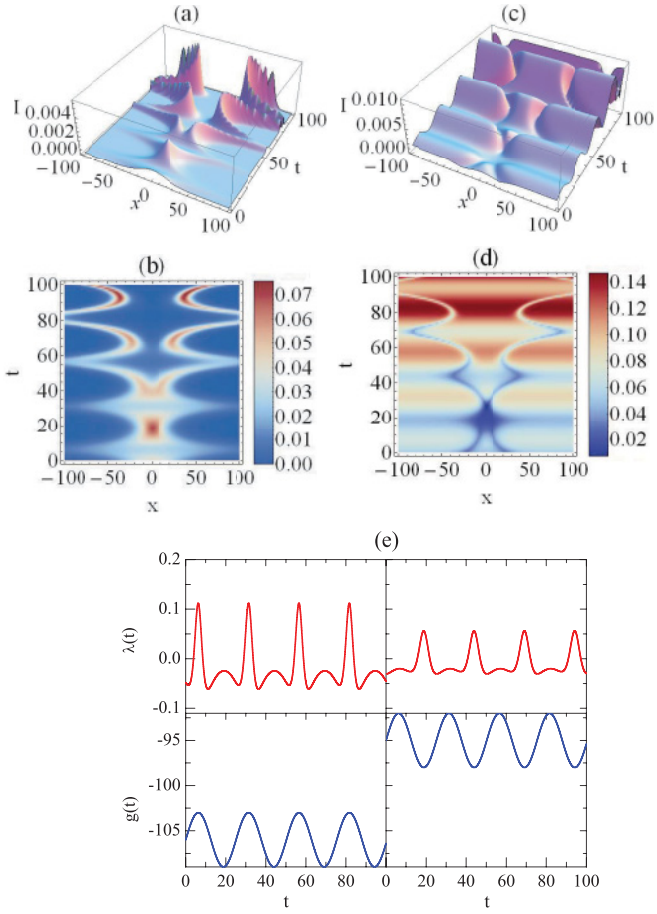

FIG. 5. (Color online) Collision dynamics between soliton pairs under interspecies interactions via Feshbach management and synchronous evolution of time-dependent external potentials in isotopic mixture with growth of condensates. The parameters used are $\gamma = 1/200$, $\Omega = 1/4$, $A = 3$, $D_1 = 1/8000$, and $D_2 = 1/800$. (a) Collision dynamics of bright-bright soliton pair with $D_4 = 2$ and $\xi = -106$. (b) Corresponding density plot for Fig. 5(a). (c) Collision dynamics of dark-dark soliton pair with $D_4 = 4$ and $\xi = -95$. (d) Corresponding density plot for Fig. 5(c). (e) Synchronous control of external harmonic potential and interaction for bright-bright soliton pair (left panel) and dark-dark soliton pair (right panel).

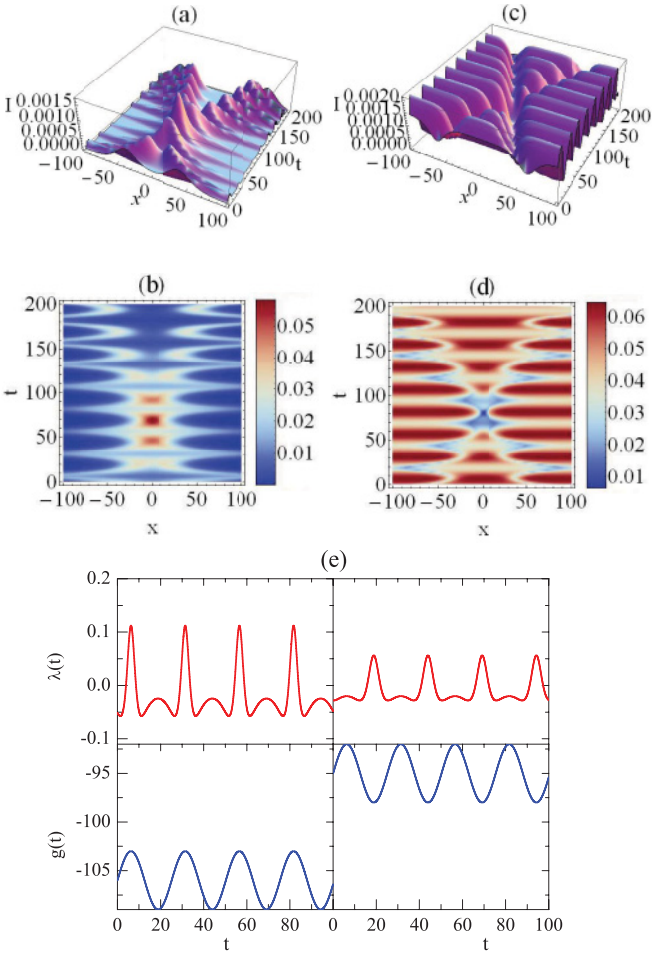

FIG. 6. (Color online) Collision dynamics between soliton pairs and synchronous change with time of external potentials in absence of the gain term. The parameters are as follows: Panels (a) and (b) show collision dynamics of bright-bright pair with $D_4 = 2$ and $\xi = -106$. Panels (c) and (d) show collision dynamics of dark-dark pair with $D_4 = 4$ and $\xi = -95$. (e) Synchronous controls of external harmonic potential and interaction for bright-bright soliton (left panel) and dark-dark soliton pairs (right panel). The other parameters used are the same as for Fig. 5.

with that in Figs. 3(a)–3(d). After the collisions, the soliton pairs in Figs. 3 and 4 show strong oscillations along their propagation directions, which are similar to those in Figs. 1 and 2. In contrast to Figs. 1 and 2, the amplitudes of the two solitons in each soliton pair are more sharply asymmetric in Figs. 3 and 4 due to different modulation schemes. As mentioned above, the soliton-pair dynamics discussed above could be realized in the present experiments. Two key steps are necessary. First, at the initial time the soliton pair should be created experimentally by possible techniques like phase imprinting, then one *synchronously* modulates the interspecies interaction and the strength of the harmonic external potential, as shown in our figures.

It is also interesting to study an isotopic system consisting of ^{85}Rb and ^{87}Rb with $\delta_{11} = 103.7$ and $\delta_{22} = 99$, which is related to those in Ref. [15]. This system has been used to investigate the phase separation in experiment and to numerically simulate the growth of dual-species BECs during simultaneous evaporative cooling [33], in which the results show that the growth of dual-species BECs during simultaneous evaporative cooling makes the condensates far from the true ground state of the system under the case of unchanged interaction and trap parameters.

In this system, ξ is taken as -106 for the bright-bright soliton pair and -95 for the dark-dark soliton pair. We explore the collision dynamics of two types of soliton pairs during the growth of two condensates are displayed in Figs. 5(a)–5(d), from which their amplitudes also increase periodically with the modulation of the interspecies interactions and harmonic external potentials, which to some extent explains the experimental phenomena in Ref. [33]. After evaporative cooling ($\gamma = 0$), the condensates are no longer growing. The collisional dynamics of soliton pairs are sequentially studied by modulating the interspecies interactions as shown in Figs. 6(a)–6(d), from which the collision times of the soliton pairs without gain are also delayed compared with

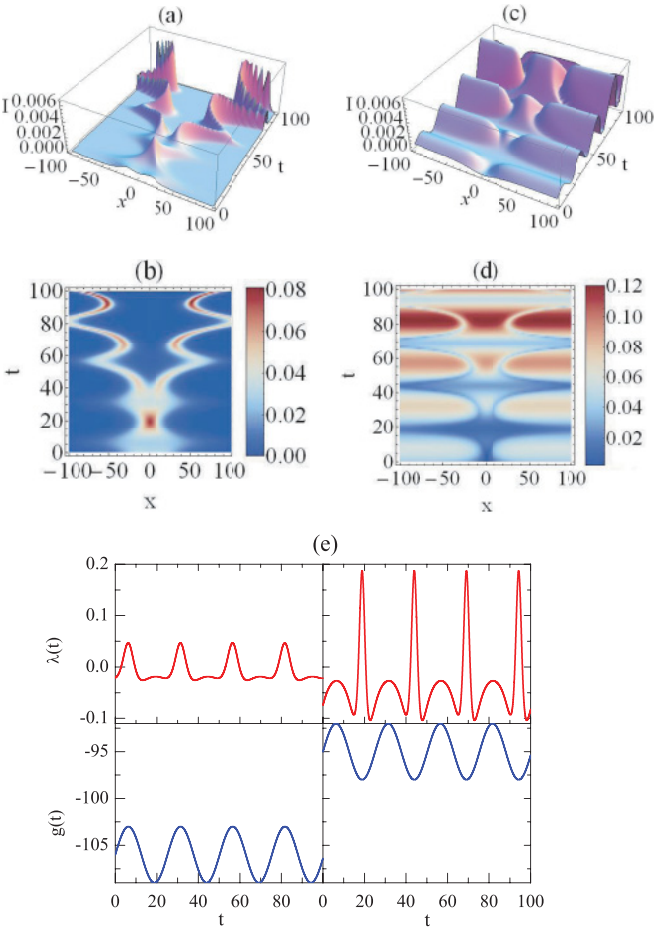

FIG. 7. (Color online) Collision dynamics between soliton pairs and synchronous change with time of external potentials in homonuclear system with gain term. The parameters are as follows: $\gamma = 1/200$, $D_1 = 1/100$, $D_2 = 1/10$, $A = 3$, and $\Omega = 1/4$. (a) Collision dynamics of bright-bright soliton pair with $D_4 = 4$ and $\xi = 106$. (b) Corresponding density plot for Fig. 7(a). (c) Collision dynamics of dark-dark soliton pair with $D_4 = 1$ and $\xi = -95$. (d) Corresponding density plot for Fig. 7(c). (e) Strengths of external potentials in upper panel and interspecies interactions in lower panel corresponding to bright-bright and dark-dark soliton ones.

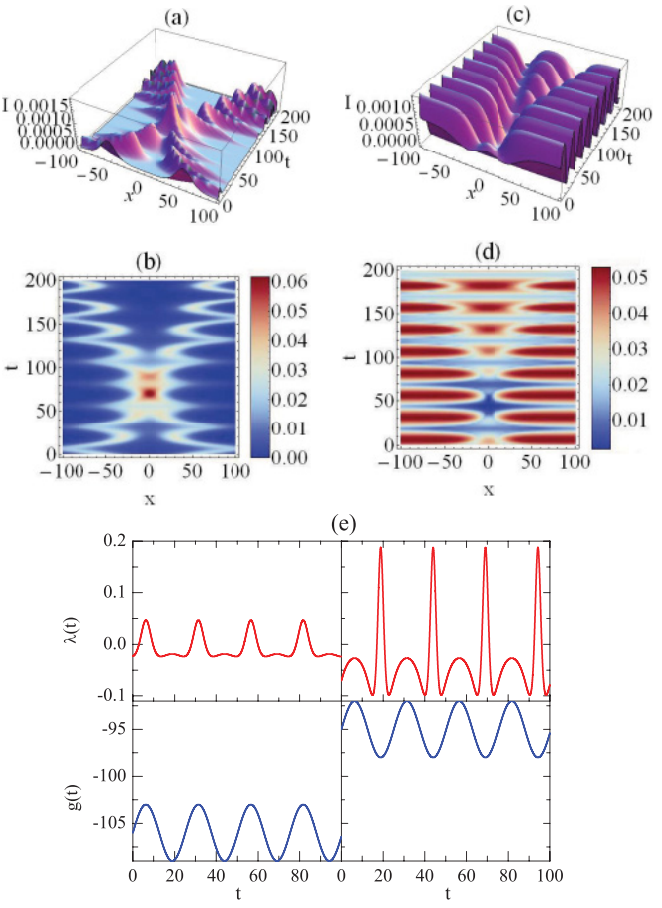

FIG. 8. (Color online) Collision dynamics between soliton pairs and evolution of relevant external potentials after stopping growth of homonuclear condensates. The parameter $\gamma = 0$ for the collision dynamics of bright-bright soltion pair [(a) and (b)] and dark-dark soliton pair in [(c) and (d)]. The other parameters are the same as those for Fig. 7. (e) Potentials and interspecies interactions for bright-bright and dark-dark soliton pairs, respectively.

those during evaporation cooling. In addition, it can be seen that the difference between the amplitudes of the two solitons in each pair only depends on the mass ratio of the two species. Because the mass ratio of ^{85}Rb and ^{87}Rb is much smaller compared with that of the heteronuclear system ^{87}Rb-^{41}K, the asymmetry between the two components is not as clear as for the two types of soliton pairs shown in Figs. 5(a), 5(d), 6(a) and 6(d) compared with those in Figs. 3(a), 3(d), 4(a) and 4(d). In Figs. 5(e) and 6(e), the left upper and lower panels of these plots show the synchronous controls of the external potential and the interspecies interaction parameters for the bright-bright soliton dynamics shown in Figs. 5(a), 5(b), 6(a) and 6(b), respectively. The controls given in the right-hand side correspond to the cases of the dark-dark soliton shown in Figs. 5(c), 5(d), 6(c) and 6(d).

From the condition Eq. (21), one can see that the strength of the external potential is related to the mass ratio, the interspecies interaction, and the gain term. Hence the different modulations of the interactions for the bright-bright and dark-dark soliton pair directly result in the distinct evolutions of the external potential, as shown in Figs. 3(e), 4(e), 5(e), and 6(e). Moreover, in comparison with Figs. 3(e) and 5(e), in Figs. 4(e) and 6(e), respectively, the external potentials are symmetric over a period of time.

In order to compare the above isotopic system with ^{85}Rb and ^{87} Rb, we consider a homonuclear system with the mixture of two different hyperfine states of ^{87}Rb and set $\delta_{22} = 99$. Because $\kappa = 1$, then $\delta_{11} = 99$. These quantities are basically close to the experimental observations. In addition, ξ is the same as that in ^{85}Rb and ^{87} Rb. In the homonuclear system, the dynamical evolution of two types of soliton pairs is shown in Figs. 7(a)–7(d) for the case of $\gamma = 1/200$ and in Figs. 8(a)–8(d) for $\gamma = 0$. It is obvious that each soliton pair is perfectly symmetric in panels (a)–(d) of Figs. 7 and 8. Their modulated interactions in the lower panels of Figs. 7(e) and 8(e) are the same as those in the lower panels of Figs. 5(e) and 6(e). However, the changes of the external potential in the upper panels of Figs. 7(e) and 8(e) are very different from those in the upper panels of Figs. 5(e) and 6(e) due to the equal masses for the two components.

V. CONCLUSION

In conclusion, we have obtained two types of solitons pairs in heteronuclear two-component BECs by the homogeneous balance principle and the F-expansion technique. We also carefully analyzed their collision dynamics under some constraint conditions with distributed parameters. The conditions can be realized in experiments by synchronous control over the interaction and the external harmonic potential parameters. In the heteronuclear systems, the obtained exact soliton-pair solutions are asymmetric, and the potentials for the two components are different, which is in sharp contrast to the homonuclear BECs. The collision dynamics of the soliton pairs and the remarkable features of collision with or without gain in heteronuclear BECs should be observed within our present experimental capacity.

ACKNOWLEDGMENTS

The work was supported by the Program for NCET, NSF, the Fundamental Research Funds for the Central Universities of China, NSFC under Grants No. 10934010, No. 60978019, and No. 11104064 and the NKBRSFC under Grants No. 2009CB930701, No. 2010CB922904, No. 2011CB921502, and No. 2012CB821300 and the NSFC-RGC under Grants No. 11061160490 and No. 1386-N-HKU748/10.

[1] M. H. Anderson, J. R. Ensher, M. R. Matthews, C. E. Wieman, and E. A. Cornell, Science **269**, 198 (1995); K. B. Davis, M. O. Mewes, M. R. Andrews, N. J. van Druten, D. S. Durfee, D. M. Kurn, and W. Ketterle, Phys. Rev. Lett. **75**, 3969 (1995); C. C. Bradley, C. A. Sackett, J. J. Tollett, and R. G. Hulet, *ibid.* **75**, 1687 (1995).

[2] D. S. Hall, M. R. Matthews, J. R. Ensher, C. E. Wieman, and E. A. Cornell, Phys. Rev. Lett. **81**, 1539 (1998).

[3] E. Timmermans, Phys. Rev. Lett. **81**, 5718 (1998).

[4] R. Navarro, R. Carretero-González, and P. G. Kevrekidis, Phys. Rev. A **80**, 023613 (2009).

[5] S. Tojo, Y. Taguchi, Y. Masuyama, T. Hayashi, H. Saito, and T. Hirano, Phys. Rev. A **82**, 033609 (2010).

[6] Th. Busch and J. R. Anglin, Phys. Rev. Lett. **87**, 010401 (2001).

[7] P. G. Kevrekidis, H. E. Nistazakis, D. J. Frantzeskakis, B. A. Malomed, and R. Carretero-González, Eur. Phys. J. D **28**, 181 (2004).

[8] V. M. Pérez-García and J. B. Beitia, Phys. Rev. A **72**, 033620 (2005).

[9] C. Becker, S. Stellmer, P. Soltan-Panhi, S. Dörscher, M. Baumert, E. Richter, J. Kronjäger, and K. Bongs, Nat. Phys. **4**, 496 (2008).

[10] X. X. Liu, H. Pu, B. Xiong, W. M. Liu, and J. B. Gong, Phys. Rev. A **79**, 013423 (2009).

[11] G. Csire, D. Schumayer, and B. Apagyi, Phys. Rev. A **82**, 063608 (2010).

[12] S. Inouye, M. R. Andrews, J. Stenger, H.-J. Miesner, D. M. Stamper-Kurn, and W. Ketterle, Nature (London) **392**, 151 (1998).

[13] A. Simoni, F. Ferlaino, G. Roati, G. Modugno, and M. Inguscio, Phys. Rev. Lett. **90**, 163202 (2003).

[14] S. B. Papp and C. E. Wieman, Phys. Rev. Lett. **97**, 180404 (2006).

[15] S. B. Papp, J. M. Pino, and C. E. Wieman, Phys. Rev. Lett. **101**, 040402 (2008).

[16] G. Thalhammer, G. Barontini, L. De Sarlo, J. Catani, F. Minardi, and M. Inguscio, Phys. Rev. Lett. **100**, 210402 (2008).

[17] P. Zhang, P. Naidon, and M. Ueda, Phys. Rev. Lett. **103**, 133202 (2009).

[18] C. J. Myatt, E. A. Burt, R. W. Ghrist, E. A. Cornell, and C. E. Wieman, Phys. Rev. Lett. **78**, 586 (1997).

[19] G. Modugno, G. Ferrari, G. Roati, R. J. Brecha, A. Simoni, and M. Inguscio, Science **294**, 1320 (2001).

[20] G. Modugno, M. Modugno, F. Riboli, G. Roati, and M. Inguscio, Phys. Rev. Lett. **89**, 190404 (2002).

[21] M. Mudrich, S. Kraft, K. Singer, R. Grimm, A. Mosk, and M. Weidemüller, Phys. Rev. Lett. **88**, 253001 (2002).

[22] M. W. Mancini, G. D. Telles, A. R. L. Caires, V. S. Bagnato, and L. G. Marcassa, Phys. Rev. Lett. **92**, 133203 (2004).

[23] K. Pilch, A. D. Lange, A. Prantner, G. Kerner, F. Ferlaino, H.-C. Nägerl, and R. Grimm, Phys. Rev. A **79**, 042718 (2009).

[24] S. Rajendran, P. Muruganandam, and M. Lakshmanan, J. Phys. B **42**, 145307 (2009); J. Math. Phys. **52**, 023515 (2011).

[25] V. I. Kruglov, A. C. Peacock, and J. D. Harvey, Phys. Rev. Lett. **90**, 113902 (2003).

[26] X. F. Zhang, X. H. Hu, X. X. Liu, and W. M. Liu, Phys. Rev. A **79**, 033630 (2009).

[27] D. S. Wang, X. H. Hu, and W. M. Liu, Phys. Rev. A **82**, 023612 (2010).

[28] Y. S. Cheng, J. Phys. B **42**, 205005 (2009).

[29] Y. B. Zhou, M. L. Wang, and T. D. Miao, Phys. Lett. A **323**, 77 (2004).

[30] Y. B. Zhou, M. L. Wang, and Y. M. Wang, Phys. Lett. A **308**, 31 (2003).

[31] W. P. Zhong, R. H. Xie, M. Belić, N. Petrović, and G. Chen, Phys. Rev. A **78**, 023821 (2008); M. Belić, N. Petrović, W. P. Zhong, R. H. Xie, and G. Chen, Phys. Rev. Lett. **101**, 123904 (2008); N. Z. Petrović, N. B. Aleksić, A. A. Bastami, and M. R. Belić, Phys. Rev. E **83**, 036609 (2011).

[32] W. P. Zhong and M. Belić, Phys. Rev. E **82**, 047601 (2010).

[33] S. Ronen, J. L. Bohn, L. E. Halmo, and M. Edwards, Phys. Rev. A **78**, 053613 (2008).